Hindawi
Advances in Materials Science and Engineering
Volume 2023, Article ID 9821983, 1 page
https://doi.org/10.1155/2023/9821983

Retraction

Retracted: Optimization of Process Parameters for Friction Stir Welding of Different Aluminum Alloys AA2618 to AA5086 by Taguchi Method

Advances in Materials Science and Engineering

Received 26 December 2023; Accepted 26 December 2023; Published 29 December 2023

This article has been retracted by Hindawi, as publisher, following an investigation undertaken by the publisher [1]. This investigation has uncovered evidence of systematic manipulation of the publication and peer-review process. We cannot, therefore, vouch for the reliability or integrity of this article.

Please note that this notice is intended solely to alert readers that the peer-review process of this article has been compromised.

Wiley and Hindawi regret that the usual quality checks did not identify these issues before publication and have since put additional measures in place to safeguard research integrity.

We wish to credit our Research Integrity and Research Publishing teams and anonymous and named external researchers and research integrity experts for contributing to this investigation.

The corresponding author, as the representative of all authors, has been given the opportunity to register their agreement or disagreement to this retraction. We have kept a record of any response received.

References

[1] G. Sasikala, V. M. Jothiprakash, B. Pant et al., "Optimization of Process Parameters for Friction Stir Welding of Different Aluminum Alloys AA2618 to AA5086 by Taguchi Method," *Advances in Materials Science and Engineering*, vol. 2022, Article ID 3808605, 9 pages, 2022.

Hindawi
Advances in Materials Science and Engineering
Volume 2022, Article ID 3808605, 9 pages
https://doi.org/10.1155/2022/3808605

Research Article

Optimization of Process Parameters for Friction Stir Welding of Different Aluminum Alloys AA2618 to AA5086 by Taguchi Method

G. Sasikala,[1] V. M. Jothiprakash,[2] Bhasker Pant,[3] R. Subalakshmi,[4] M. Thirumal Azhagan,[5] K. Arul ,[6] Wadi B. Alonazi,[7] M. Karnan,[8] and S. Praveen Kumar [9]

[1]*Department of Mathematics, SRM Valliammai Engineering College, Kattankulathur, Chennai 603202, Tamil Nadu, India*
[2]*Department of Mechanical Engineering, Easwari Engineering College (Autonomous), Ramapuram, Chennai 600 089, Tamil Nadu, India*
[3]*Department of Computer Science & Engineering, Graphic Era Deemed to be University, Dehradun, Uttarakhand 248002, India*
[4]*Department of Civil Engineering, Sri Sairam Engineering College, Chennai, Tamil Nadu 600044, India*
[5]*Department of Production Technology, Madras Institute of Technology, Anna University, Chennai, Tamil Nadu 600044, India*
[6]*Department of Mechanical Engineering, Agni College of Technology, Chennai 603 103, Tamil Nadu, India*
[7]*Health Administration Department, College of Business Administration, King Saud University, PO Box 71115, Riyadh 11587, Saudi Arabia*
[8]*Grassland and Forage Division, National Institute of Animal Science, Cheonan-si, Chungcheongnam-do 31000, Republic of Korea*
[9]*Department of Mechanical Engineering, Faculty of Mechanical Engineering, Arba Minch Institute of Technology (AMIT), Arba Minch University, Arba Minch, Ethiopia*

Correspondence should be addressed to S. Praveen Kumar; praveen.kumar@amu.edu.et

Received 3 December 2021; Accepted 3 January 2022; Published 15 February 2022

Academic Editor: Palanivel Velmurugan

Friction stir welding (FSW) was used to combine two different Al–Cu alloys, AA2618-T87 and Al–Mg alloy AA5086-H321 plates, and the characteristics of the procedure were adjusted using Taguchi L16 orthogonal experiments planned in advance. Consideration was given to a variety of factors including rotational and cross-sectional speeds, geometry, and the tool-to-pin-diameter ratio. The tensile strength of the joint was used to identify the best procedure parameters. Runs with the ideal settings confirmed the projected optimal tensile strength value. A wide range of process parameters can be used to generate high-quality joints, according to this study. According to the results of an analysis of variance, the most important factor in determining the soundness of a joint is the fraction of tool contact area to pin diameter, although pin shape and welding speed also have a major impact. During this examination, it was observed that the nugget region is dominated by material on the forward-moving side. Heat-affected zones with tensile failures occurred on the alloy 5086 side of the weldment.

1. Introduction

There are many difficulties associated with welding dissimilar alminium alloys, mainly because the constituent elements create low melting eutectics (hot cracking) [1]. Weld metal composition is highly dependent on the filler metal, base metal, and quantity of dilution when it comes to solidification cracking in aluminum alloys [2, 3]. For the weld connection to be free of solidification cracks, the filler composition and/or welding parameters must be carefully selected. This may be done easily using fusion welding aluminum alloys. Depending on the aluminum alloy, filler metals can be selected in a variety of ways [4]. Fusion welding of different aluminum alloys presents a challenge in terms of dealing with solidification cracking. There are no filler metals that can create crack-free welding for many aluminum alloy combinations [5–7]. When filler metal is available, joint efficiency can not be achieved even if the metal is of adequate quality. Fusion welding of different

aluminum alloys is often discouraged in the industry because of these reasons [8].

Welding different aluminum alloys is best done using solid-state welding methods. There is no need to worry about weld solidification cracking because these methods do not require melting [9–11]. Using solid-state welding procedures, these problems with pores, dispersion, fragile intermetallic creation, and heat influenced zone liquation cracking in aluminum alloy fusion welding can be avoided [12]. Welding dissimilar aluminum alloys can be done via friction stir welding to create butt joints and other custom-designed weld joint types. As a result of its engineering importance and challenges connected with traditional welding, FSW has been the subject of a lot of academic studies [13, 14]. Friction stir welding (FSW) is a type of solid-state welding. It is frequently referred to as a sort of friction welding, but it is regarded as a different welding technique due to its many uses. There is no external heat in this welding process, and the joint formation occurs due to diffusion at interface surfaces under high pressure and friction force. Because there is no molten or plastic state involved in this process, it is classified as a solid-state welding technique.

Welding a range of aluminum alloys combined with FSW has been done before, with outstanding results. As in most of these studies, the Stir Zone (SZ) or Weld Nugget Zone (WZ) showed substantial mechanical mixing with a complicated vortex of two alloys [15]. The position of two different alloys has been found to have a significant impact on the flow of material and the quality of welds [16]. In many studies, experts have shown that it is better to place one of the two materials on the side that is moving forward. Cast aluminum alloy A356 was discovered to have a much higher SZ than wrought aluminum alloy AA6061 when compared to the FSW of the two alloys [17]. In the SZ during the FSW of the transition from AA2618 to AA6061, the material on the advancing side was most common. Aside from material flow visualization, there was no optimal FSW parameter or tool geometry found in these systems in these investigations [18, 19].

1.1. FSW Parameters. With a quasiroller, pins and shoulders are intertwined with each other at their opposite ends, in which the joint line is traveled along the lateral aspect. The tool is used to manipulate the material and heat it to create the joint [20–22]. It is used to heat the workpiece by using friction and plastic deformation between the instrument and the object being worked on. Heating around the pin softens the surrounding material while a mix of tool rotation and translation is used [23]. This technique results in a strong joint. Because of the instrument's multiple geometrical features, the flow of material around the pin might be somewhat difficult. Due to FSW, fine and equiaxed recrystallized grains are formed in the material because of plastic deformation at high temperatures [24, 25]. FSW have good mechanical properties because of their fine microstructure. Listed below is a complete breakdown of the various factors that go into the FSW process:

(1) The tool's speed of rotation (rpm).

(2) Welding speed in the transverse direction. (mm/min).

(3) A piece of equipment's form.

  (a) Pin profile.
  (b) Size of the tool's shoulder, D (mm).
  (c) Size of the pin, d (mm).
  (d) D/d ratio of the tool.
  (e) The length of the pin (mm).
  (f) inclination of the tool

Equipment geometry, speed of rotation, and other factors have been studied and found to have a substantial impact on the quality of welds in FSW. A perfectly executed weld between the dissimilar metals AA5052 and AA2017 has been reported to be possible at transverse speeds of 60 mm/min and rotation speeds of 1000 rpm, according to the available information. Furthermore, the fracture toughness of the material increases directly to the welding speed. Then it starts to fall. Due to the rare, irregularly created voids along the base metal/weld zone boundary on the advancing side. Weld flaws are common at high rotating speeds. On the advancing side, there are irregularly formed voids along the base metal/weld zone border. At high rotational speeds, weld defects are also typical.

To compare rotational speeds for friction, stir welding of AA8009, [26]observed at 1200 revolutions per minute, the fracture toughness was 60–70% that of the basic metal and 90% at 428 rpm, in their investigations. Elangovan et al. [18] found that when the more durable foundation was positioned on the forward-moving side, the nugget region was properly mixed. When welding with poorer material, the weld nugget was much thinner and there was insufficient mixing. According to the information shown above, successful dissimilar friction stir welding necessitates using good judgement when deciding where to position the materials, developing the tools, and adjusting the process parameters according to on the joining materials' qualities.

Figure 1 reveals the schematic diagram of Friction stir welding. Aluminum alloys with copper and magnesium, such as AA2618 and AA5086, are common in the aircraft sector. When Cu and Mg are combined in a liquid state, a low melting eutectic is formed, resulting in solidification cracking. Using fusion welding on these alloys is not an option. When it comes to combining different metals and alloys, friction stir welding has been examined by scientists in the past few years. With good joint efficiency, FSW has effectively combined a variety of options of aluminum alloys. A significant amount of magnesium is used in the 5000 series alloys. Strength and corrosion resistance in seawater can be achieved with a magnesium content of 5% or more. FSW is almost unexplored for this particular set of materials. AA5086 is weldable with FSW because of this. Data for the four factors studied, the transversal speed in addition to the speed of rotation, the shape of a tool pin, and the D/d ratio are tabulated in Table 1. Table 2 reveals the alloys' chemical composition (weight percent). Figure 2 reveals the welded sample.

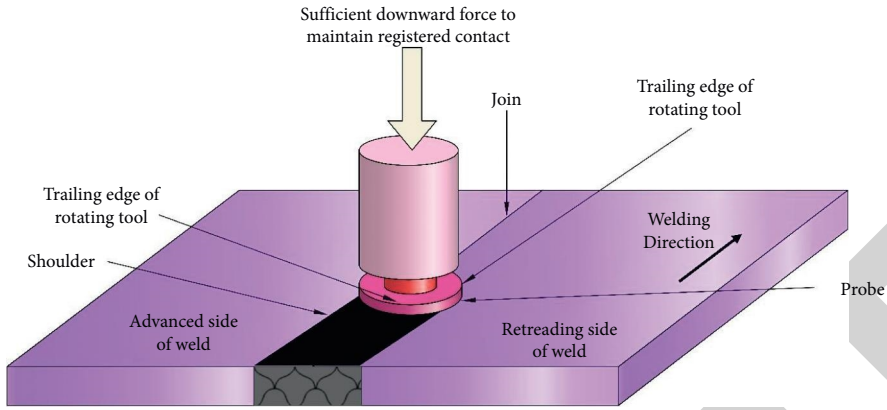

Figure 1: Schematic Diagram of Friction stir welding.

Table 1: The values and levels of each of the four performance characteristics.

Levels	Tool pin geometry	Rotational speed	Transverse speed	Ratio
1	Straight cylinder	450	15	2
2	Tapered cylinder	600	35	2.5
3	Cylindrical threaded	750	50	2.75
4	Tapered threaded	850	65	3

Table 2: The alloys chemical composition (weight percent).

Material	Mg	Mn	Fe	Si	Cu
AA5086	4.5	0.7	0.31	0.4	0.1
AA2618	1.5	1	0.13	0.01	4.0

1.2. Taguchi Method. Quality assurance, both on and off-line, is two of Taguchi's main areas of focus. A typical experimental design focuses primarily solely on the average quality of the data, but Taguchi is considered as the core design, the minimizing of the characteristic of interest's variation. However, despite its many flaws, the Taguchi approach now has an excellent job of solving single response issues. The purpose of robust design is to create a product that never fails to perform its intended function during its useful life. The Taguchi technique, widely known as robust design methodology, provides a method for developing requirements for complete design utilizing the design of experiments theory. Using the Taguchi approach, a process or product design can be improved through the three stages:

(1) Designing a concept or a system.

(2) Design of parameters.

(3) Design with a degree of slack.

The following enumerated items are measures that must be taken in order to optimize the process parameters.

Step 1: The quality attribute to be optimized must be determined.

Step 2: Remain aware of the noise components and test conditions that could influence the results.

Step 3: Determine the variables under control and the range of possible values for each.

Step 4: The data analysis technique should be defined in conjunction with the matrix experiment design.

Step 5: Perform the matrices test.

Step 6: Data analysis is necessary to identify optimal levels for control parameters.

Step 7: At these criteria, estimate the outcomes.

1.3. The Decision of an Orthogonal Array (OA). These factors are listed in ascending order of importance when deciding which orthogonal array to utilize:

(1) Quantity of products and interconnections that are relevant

(2) Factors of interest that have a certain number of levels

(3) Cost constraints or the required experimental resolution

L16 OA is chosen in this study because four levels and four components are taken into account. The interactions between factors are not taken into account. In order to get a total of 12 degrees of freedom (Dof), each aspect has a degree of freedom of 3 (No. Of levels 1, i.e., 4 1 = 3). A good rule of thumb is that the OA's dof should be bigger than all other factor dofs combined on average. L16's dof is 15, which makes it eligible for the study. Table 3 detail the plate's mechanical characteristics.

Figure 2: Welded sample.

Table 3: Materials' mechanical characteristics.

Metal	Proof strength at 0.2% (MPa)	Ultimate tensile strength (MPa)	Percentage of elongation
AA5086	268	320	31
AA2618	400	488	22

2. Experimental Procedure

In this project, Al-Cu alloy AA2618-T87 and Al-Mg alloy AA5086-H321 sheets with a thickness of 6 mm were utilized. It was cut into rectangular coupons (160 mm in length and 70 in width) for friction stir welding from rolled plates. Using a FSW process, the butt joints were welded. The butt joints were constructed in the same direction as the rolling. The trials were carried out utilizing the design parameters, L16 OA. A better approach with process parameters is with rotor velocity, spindle speed, pin profile, and D/d ratio. These are all good starting points. For friction stir welding, H13 grade tool steel (5.7 mm pin span and 12 mm pin radius) was employed. Joint lines were aligned, and a little pin was placed in each one. Figure 3 reveals the tensile specimen's dimensions. Samples were made welding coupons in their final, as-welded state, each with an overall length of 100 millimetres (25 mm gauge length x 6 mm width). Universal tensile testing equipment was used to conduct tensile tests on three materials at room temperature in accordance with ASTM E8 [32]. The smooth profile tensile specimens were cut using a wire cut EDM. Three specimens were made for each level of the planned matrix in order to minimize the machining error (noise). These samples were tested for their tensile strength, and the results were published. It is shown in Table 4 that the experiment was successful. As-welded welds were examined for microstructure. For 15 seconds, a force of 100 g was applied to the weldment to measure Vickers microhardness data.

3. Results and Discussion

The quality of the intended qualities is calculated as a percentage of the SN ratio. As structural rigidity is the primary objective, the higher the SN ratio, the better the outcomes. The method of computing the SN ratio is presented as follows:

$$\frac{S}{N\,\text{ratio}}(\eta) = -10\log_{10}\frac{1}{n}\sum_{i=1}^{n}\frac{1}{y_i^2}. \quad (1)$$

FSW joint tensile strength is measured in order to better understand the FSW process. Experimental data is used in order to compute both mean and standard deviation (SN) as shown in Table 4. For each level, the average mean and SN ratio are shown in Tables 5 and 6. Higher SN Ratios indicate better quality. A3, B3, C1, and D4 are the best choices based on mean and SN ratios.

3.1. Analysis of Variance (ANOVA). Analysis of Variance is a technique that identifies which variables are statistically significant. So you can see just how much the process parameter influences your reaction and how significant it is. There are ANOVA tables in Tables 7 and 8 for the mean and the noise to signal ratio. In terms of the mean and SN ratio, the results are shown in Figures 4 and 5. The F test is being used to determine the performance parameters that are of immense value in this study. An F value that is higher indicates that the factor has a greater impact on the outcome of the process. We discovered that the D/d ratio had a substantial impact on the tensile strength of the weld throughout our investigation.

3.2. Toughness Estimation of Tensile Strength. A_3., B_3., C_1., D_4. are the best settings for the experiment. According to the literature, we use a tensile strength prediction using an additive modelling approach. Table 4 displays the average values for each of the components at the various levels.

Based on the mean, these are the best parameters to use. $A_3B_3C_1D_4$.

Based on the SN ratio, these are the best parameters to use. $A_3B_3C_1D_4$.

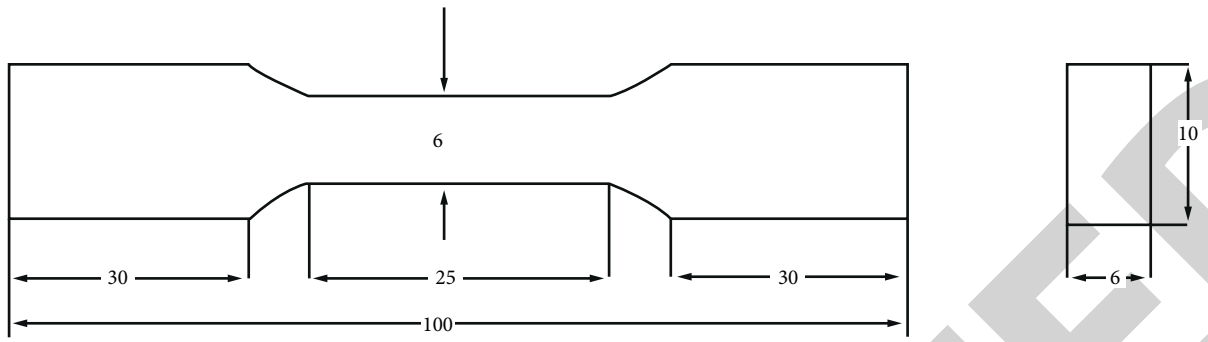

Figure 3: Tensile specimen's dimensions.

Table 4: L16 orthogonal array with a mean value and SN ratio measurement.

S.No	A tool pin geometry	B rotational speed	C transverse speed	D D/d ratio	Mean tensile strength (MPa)	SN ratio
1	1	1	1	1	105	40.4750
2	1	2	2	2	240	47.5798
3	1	3	3	3	248	47.8815
4	1	4	4	4	159	43.9851
5	2	1	2	3	204	46.1941
6	2	2	1	4	263	48.3926
7	2	3	4	1	105	40.3889
8	2	4	3	2	116	41.2504
9	3	1	3	4	289	49.2144
10	3	2	4	3	279	48.9159
11	3	3	1	2	277	48.8549
12	3	4	2	1	127	42.0312
13	4	1	4	2	299	49.4958
14	4	2	3	1	102	40.1050
15	4	3	2	4	291	49.2625
16	4	4	1	3	247	47.8358

Table 5: Means values.

Level	A	B	C	D
1	192	231	231	110
2	178.6	228	229	241
3	251	240	196	252
4	246	178	219	259
Delta	82	76.3	35.4	149
Rank	2	3	4	1

Table 6: SNR (signal to noise ratio).

Level	A	B	C	D
1	47.8	47.4	48	41
2	45.2	49.2	48.1	48.1
3	49.6	48	46	47.4
4	47.4	46.2	44	4.6
Delta	4.1	3.1	2.1	7.2
Rank	2	3	4	1

3.3. Confirmation Run. The cylindrically threaded pin profile was used in the confirmation studies. Other parameters were set to their optimum values as well. The spinning speed was set to 750 rpm, the transversal speed to 15 mm/min, and the D/d ratio was adjusted to 3. It was found that the average compressive strength of the FSW specimens AA2618 and AA5086 was 301 MPa.

Particles of second-phase intermetallic were found in both of the materials used in the research. Iron/manganese aluminides were found in alloy 5086's second-phase

Table 7: Means-variance analysis.

Source	Degrees of freedom	Seq SS	Adj MS		% Contribution
A	3	14428.6	4812.124	0.81	15.81
B	3	12168.2	4128.41	0.51	14.12
C	3	26.41.2	861.1312	0.22	2.16
D	3	52471.6	17817.34	4.71	61.50
Residual error	3	5681.3	1871.7		6.1284
Total	15	81342.1			100

Table 8: Statistical ANOVA for the correlation between signal and noise.

Source	Degrees of freedom	Sequential sum of squares	Adjusted mean square	Fisher ratio	Contribution percentage
A	3	21.28	7.6829	0.51	13.142
B	3	19.81	6.91284	0.39	9.9582
C	3	6.82	2.4283	0.41	4.186124
D	3	128.546	41.2838	7.16	69.5428
Residual error	3	11.812	3.9426		5.4823
Total	15	201.428			100

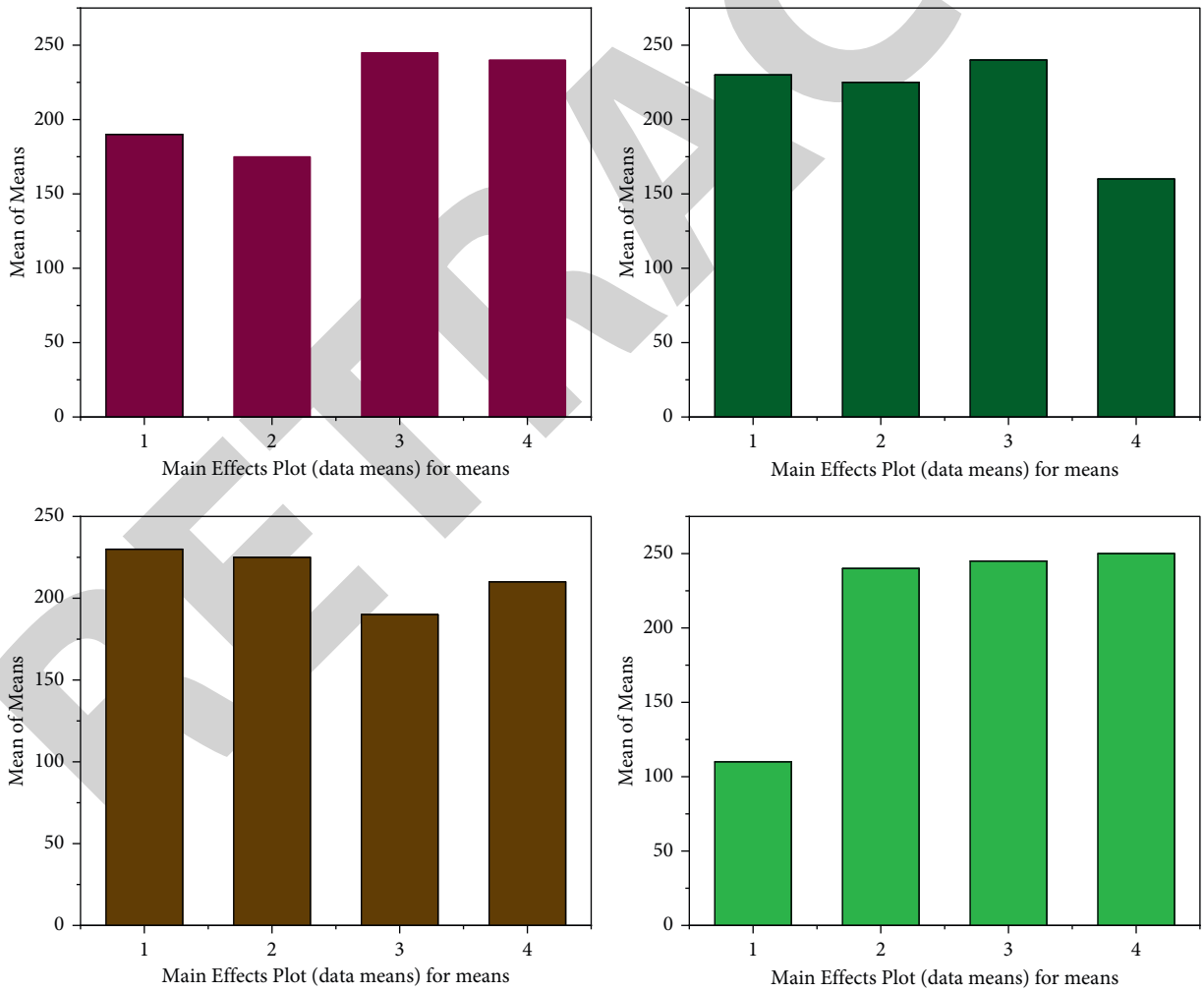

Figure 4: Main effects of the plot for mean.

particles, while eutectic Al-2Cu (θ) particles were found in alloy 2618. Particles in the alloy's second phase 5086 were smaller and finer than those in alloy 2618. The weld contained three unique microstructural zones: SZ, TMAZ, and HAZ. There was a clearly defined SZ/TMAZ and TMAZ/HAZ boundary on the forward-moving side of the

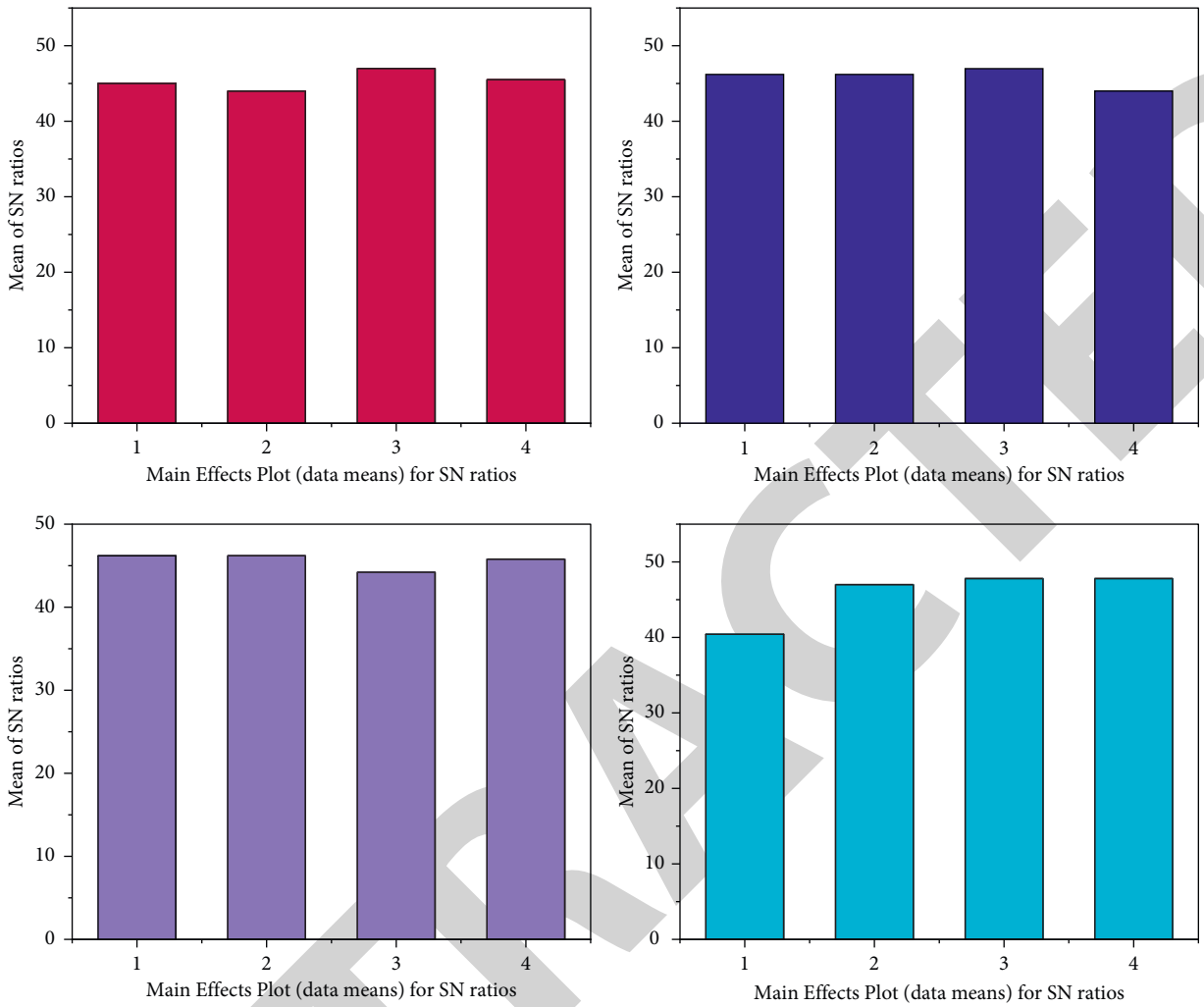

Figure 5: Main effects of the plot for SN ratio.

TMAZ. Dispersion of these contacts was greater on the retreating side. Compared to the foundation materials that were not affected, the grain structure of the weld nugget did not appear to have changed significantly in the HAZ. For the purpose of identifying any differences in properties between the various areas of the weld, Vickers microhardness tests were performed at 0.25 mm intervals across the weld. Using unmodified 2618, the hardness of the weld nugget boundaries was reduced considerably. Because the weld nugget was softer than the 2618 base material, its hardness was significantly lower. Relative to the 5086 base material, the hardness of the weld nugget retreating side was just marginally reduced. A 5086 basic material is compared, the weld nugget had a higher hardness. Base material 2618 had a much greater hardness rating than 2618 base material, which is predicted.

On the 5086-side HAZ, all three weld specimens failed. Figure 6 depicts the welding microhardness profile. Compared to alloy 5086, alloy 2618 has a much higher strength. Welded specimens were significantly stronger than those made of the 5086 basic material.

FSW was discovered to be the case to make acceptable butt welds between the two aluminum alloys studied, proving its ability to weld incompatible aluminum alloys. Even though FSW of aluminum alloys from different families has been established in several previous studies, one unique element of the welds formed in this work is insufficient metal mixing to cause significant corrosion. Similarly, friction stir welds between alloys 5086 and 6061 had comparable findings. "Chaotic mixing" welding two different metals together was reported in numerous earlier experiments. In addition, it was found that the onion rings had alternating layers of the two metals. Materials positioned closer to the nuggets are more likely to be dragged into them. Friction Stir On the substrate surface of a weld, temperatures rise, and deformations are more significant than on the receding side. Based on what we have learned so far, further investigation is needed to explain this observation fully. Positioning the more robust base material forward increases joint efficiency in any case.

To determine whether a weld qualifies for dissimilar welding, the lower one base material should fail out of the

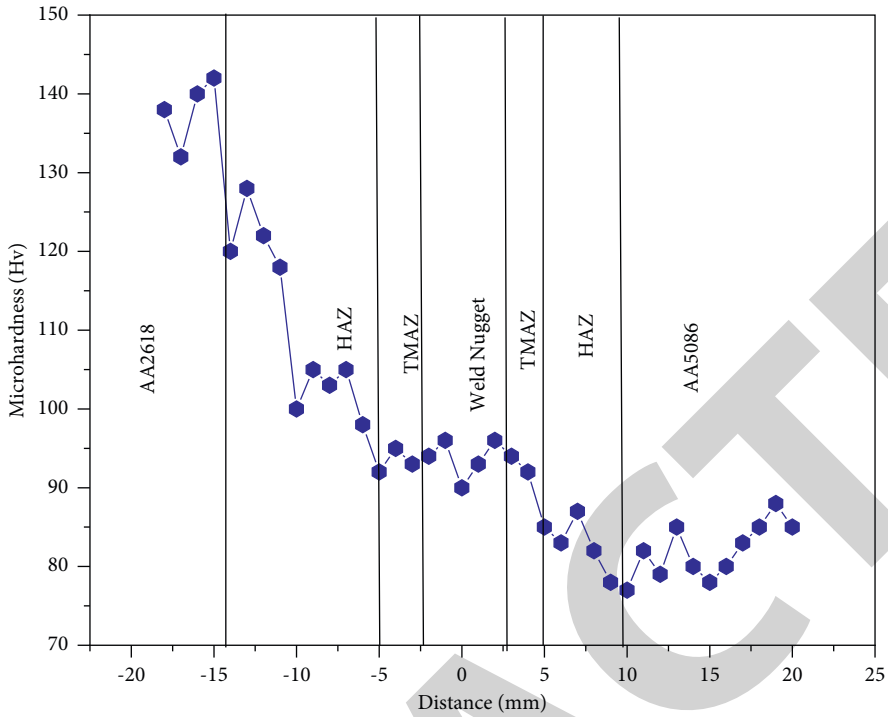

Figure 6: Welding microhardness profile.

way of the joint. All of the failures occurred on the 5086-side of the weldment, which has the lowest hardness ratings, due to friction stir welding. Only significantly less intense than 5086-H321 base material specimens were weld specimens. Due to annealing effects, cold work in the HAZ may have been lost. FSW achieves a junction efficiency of over 90% (based on alloy AA5086), significantly more significant than the standard fusion welding procedure can accomplish.

4. Conclusions

The ultimate tensile strength was taken into account for optimizing FSW process parameters. The spindle speed is 700 rpm, the transversal speed is 15 mm/min, and the D/d ratio is 3. When tool profiles were compared, the cylindrical threaded pin tool profile won. The D/d ratio accounts for 60% of the overall contribution, essential. FSW has a connection effectiveness of 90% and may be used to join AA2618-T87 and AA5086-H321 sheets, 5086 Alloy (based on AA5086). This material combination occurs in the heat-affected zone of Alloy 5086. The best parameters are tool pin geometry (*A*)–15.81 percent, rotational speed (B)–14.12 percent, transverse speed (C)–2.16 percent, D/d ratio (*D*)–61.50 percent, and the best parameters are $A_3B_3C_1D_4$.

Data Availability

The data used to support the findings of this study are included in the article. Should further data or information be required, these are available from the corresponding author upon request.

Conflicts of Interest

The authors declare that there are no conflicts of interest regarding the publication of this paper.

Acknowledgments

The authors thank Sri Sairam Engineering College, Chennai, and SRM Valliammai Engineering College, Chennai, for providing technical assistance to complete this experimental work. This project was supported by Researchers Supporting Project number (RSP-2021/332) King Saud University, Riyadh, Saudi Arabia.

References

[1] S. T. Amancio-Filho, S. Sheikhi, J. F. Dos Santos, and C. Bolfarini, "Preliminary study on the microstructure and mechanical properties of dissimilar friction stir welds in aircraft aluminium alloys 2024-T351 and 6056-T4," *Journal of Materials Processing Technology*, vol. 206, no. 1–3, pp. 132–142, 2008.

[2] K. S. A. Ali, V. Mohanavel, S. A. Vendan et al., "Mechanical and microstructural characterization of friction stir welded SiC and B4C reinforced aluminium alloy AA6061 metal matrix composites," *Materials*, vol. 14, no. 11, Article ID 3110, 2021.

[3] R. Priya, V. Subramanya Sarma, and K. Prasad Rao, "Effect of post weld heat treatment on the microstructure and tensile properties of dissimilar friction stir welded AA 2219 and AA 6061 alloys," *Transactions of the Indian Institute of Metals*, vol. 62, no. 1, pp. 11–19, 2009.

[4] R. S. Mishra and Z. Y. Ma, "Friction stir welding and processing," *Materials Science and Engineering: R: Reports*, vol. 50, no. 1–2, pp. 1–78, 2005.

[5] L. E. Murr, Y. Li, R. D. Flores, E. A. Trillo, and J. C. McClure, "Intercalation vortices and related microstructural features in the friction-stir welding of dissimilar metals," *Materials Research Innovations*, vol. 2, no. 3, pp. 150–163, 1998.

[6] W.-B. Lee, Y.-M. Yeon, and S.-B. Jung, "The joint properties of dissimilar formed Al alloys by friction stir welding according to the fixed location of materials," *Scripta Materialia*, vol. 49, no. 5, pp. 423–428, 2003.

[7] I. Shigematsu, Y.-J. Kwon, K. Suzuki, T. Imai, and N. Saito, "Joining of 5083 and 6061 aluminum alloys by friction stir welding," *Journal of Materials Science Letters*, vol. 22, no. 5, pp. 353–356, 2003.

[8] Y. Li, L. E. Murr, and J. C. McClure, "Flow visualization and residual microstructures associated with the friction-stir welding of 2024 aluminum to 6061 aluminum," *Mater. Sci. Eng. A*, vol. 271, no. 1–2, pp. 213–223, 1999.

[9] P. Cavaliere and F. Panella, "Effect of tool position on the fatigue properties of dissimilar 2024-7075 sheets joined by friction stir welding," *Journal of Materials Processing Technology*, vol. 206, no. 1–3, pp. 249–255, 2008.

[10] C. G. Rhodes, M. W. Mahoney, W. H. Bingel, R. A. Spurling, and C. C. Bampton, "Effects of friction stir welding on microstructure of 7075 aluminum," *Scripta Materialia*, vol. 36, no. 1, pp. 69–75, 1997.

[11] H. Fujii, L. Cui, M. Maeda, and K. Nogi, "Effect of tool shape on mechanical properties and microstructure of friction stir welded aluminum alloys," *Mater. Sci. Eng. A*, vol. 419, no. 1–2, pp. 25–31, 2006.

[12] W.-k. Kim, B.-c. Goo, and S.-t. Won, "Optimal design of friction stir welding process to improve tensile force of the joint of A6005 extrusion," *Materials and Manufacturing Processes*, vol. 25, no. 7, pp. 637–643, 2010.

[13] A. K. Lakshminarayanan and V. Balasubramanian, "Process parameters optimization for friction stir welding of RDE-40 aluminium alloy using Taguchi technique," *Transactions of Nonferrous Metals Society of China*, vol. 18, no. 3, pp. 548–554, 2008.

[14] S. Vijayan, R. Raju, K. Subbaiah, N. Sridhar, and S. R. K. Rao, "Friction stir welding of Al-mg alloy optimization of process parameters using Taguchi method," *Experimental Techniques*, vol. 34, no. 5, pp. 37–44, 2010.

[15] S. Vijayan, R. Raju, and S. R. K. Rao, "Multiobjective optimization of friction stir welding process parameters on aluminum alloy AA 5083 using Taguchi-based grey relation analysis," *Materials and Manufacturing Processes*, vol. 25, no. 11, pp. 1206–1212, 2010.

[16] G. D'urso and C. Giardini, "The influence of process parameters and tool geometry on mechanical properties of friction stir welded aluminum lap joints," *International Journal of Material Forming*, vol. 3, no. 1, pp. 1011–1014, 2010.

[17] T. P. Chen and W.-B. Lin, "Optimal FSW process parameters for interface and welded zone toughness of dissimilar aluminium-steel joint," *Science and Technology of Welding & Joining*, vol. 15, no. 4, pp. 279–285, 2010.

[18] K. Elangovan, V. Balasubramanian, and M. Valliappan, "Influences of tool pin profile and axial force on the formation of friction stir processing zone in AA6061 aluminium alloy," *International Journal of Advanced Manufacturing Technology*, vol. 38, no. 3–4, pp. 285–295, 2008.

[19] T. Chen, "Process parameters study on FSW joint of dissimilar metals for aluminum-steel," *Journal of Materials Science*, vol. 44, no. 10, pp. 2573–2580, 2009.

[20] R. Karthikeyan and V. Balasubramanian, "Predictions of the optimized friction stir spot welding process parameters for joining AA2024 aluminum alloy using RSM," *International Journal of Advanced Manufacturing Technology*, vol. 51, no. 1, pp. 173–183, 2010.

[21] W. A. Baeslack, K. V. Jata, and T. J. Lienert, "Structure, properties and fracture of friction stir welds in a high-temperature Al-8.5Fe-1.3V-1.7Si alloy (AA-8009)," *Journal of Materials Science*, vol. 41, no. 10, pp. 2939–2951, 2006.

[22] S.-K. Park, S.-T. Hong, J.-H. Park, K.-Y. Park, Y.-J. Kwon, and H.-J. Son, "Effect of material locations on properties of friction stir welding joints of dissimilar aluminium alloys," *Science and Technology of Welding & Joining*, vol. 15, no. 4, pp. 331–336, 2010.

[23] R. Nandan, T. DebRoy, and H. Bhadeshia, "Recent advances in friction-stir welding - process, weldment structure and properties," *Progress in Materials Science*, vol. 53, no. 6, pp. 980–1023, 2008.

[24] P. J. Ross, *Taguchi Techniques for Quality Engineering: Loss Function, Orthogonal Experiments, Parameter and Tolerance Design*, McGraw Hill Professional, New York, NY, USA, 2nd edition, 1996.

[25] S. Datta, A. Bandyopadhyay, and P. K. Pal, "Application of Taguchi philosophy for parametric optimization of bead geometry and HAZ width in submerged arc welding using a mixture of fresh flux and fused flux," *International Journal of Advanced Manufacturing Technology*, vol. 36, no. 7–8, pp. 689–698, 2008.

[26] P. B. Srinivasan, W. Dietzel, R. Zettler, J. F. Dos Santos, and V. Sivan, "Stress corrosion cracking susceptibility of friction stir welded AA7075–AA6056 dissimilar joint," *Materials Science and Engineering: A*, vol. 392, no. 1–2, pp. 292–300, 2005.